

# Contribution of $^1\text{H}$ combined rotation and multipulse spectroscopy nuclear magnetic resonance to the study of tricalcium silicate hydration

B. BRESSON, H. ZANNI, S. MASSE

*Laboratoire de Physique et Mécanique des Milieux Hétérogènes,  
Unité de Recherche associée au CNRS 857, Ecole Supérieure de Physique et Chimie  
Industrielle, 10 rue Vauquelin, 75005 Paris, France*

C. NOIK

*Institut Français du Pétrole, 1–4 avenue de Bois Préau, 92506 Rueil-Malmaison, France*

Hydration products of tricalcium silicate ( $\text{C}_3\text{S}$ ) are the calcium silicate hydrates (C–S–H) and portlandite. Silica fume, added to anhydrous cement in industrial formulations, reacts with portlandite and leads to C–S–H slightly different from the previous one (this reaction is called the pozzolanic reaction).  $\text{C}_3\text{S}$  hydration at  $120^\circ\text{C}$  with and without silica fume has been studied by two  $^1\text{H}$  nuclear magnetic resonance techniques: combined rotation and multipulse spectroscopy (CRAMPS) and magic angle spinning (MAS). The static spectra are broadened by the proton–proton dipolar interaction. The  $^1\text{H}$  MAS technique does not allow us to remove the effects of this interaction completely and cannot be in this case a quantitative method. Therefore the CRAMPS technique, which can remove the broadening of the interaction because of the use of a multipulse sequence associated with the sample rotation, was used. It is shown that the CRAMPS NMR spectra allow us to describe the action of silica fume on the hydrates and to reveal the competition between portlandite formation around the  $\text{C}_3\text{S}$  grains and portlandite dissolution near the silica grains until the complete dissolution of portlandite.

## 1. Introduction

Tricalcium silicate ( $\text{C}_3\text{S}$ ) is the major component of Portland cement (cement chemists' notation: C = CaO; S =  $\text{SiO}_2$ ; H =  $\text{H}_2\text{O}$ ). At room temperature, the products formed during the  $\text{C}_3\text{S}$  hydration are the calcium silicate hydrates (C–S–H) which are non-crystalline systems, and portlandite ( $\text{Ca}(\text{OH})_2$ ), which is a crystalline phase. At higher temperatures (typically  $120^\circ\text{C}$ ), the hydration reaction is accelerated and C–S–H crystalline phases can appear [1].

In the last 10 years, the hydration products of  $\text{C}_3\text{S}$  were widely studied by solid-state  $^{29}\text{Si}$  magic angle spinning (MAS) nuclear magnetic resonance (NMR) in single-pulse or cross-polarization experiments [2]. The  $^{29}\text{Si}$  NMR allows us to determine the silicate skeleton of the hydrates. It is now well established that the structure is based on  $\text{SiO}_4$  tetrahedra chains. As an example, the  $^{29}\text{Si}$  single-pulse spectrum of  $\text{C}_3\text{S}$  hydrated at  $120^\circ\text{C}$  for 24 h is shown in Fig. 1.  $^{29}\text{Si}$  NMR spectra are analysed using the  $Q_n$  classification, where Q stands for the  $\text{SiO}_4$  tetrahedron and  $n$  refers to the number of tetrahedra linked by oxygen bonds to the previous tetrahedron. Thus,  $n$  varies from 0 to 4.  $Q_2$ ,

which is a tetrahedron linked with two neighbouring tetrahedra, is a middle-chain site.  $Q_1$  is an end-chain site.  $Q_0$  is a monomeric site. The peaks located between  $-65$  and  $-75$  ppm correspond to a  $Q_0$  entity, characteristic of anhydrous unreacted material and the peaks located around  $-80$  and  $-85$  ppm correspond to  $Q_1$  and  $Q_2$  entities, respectively, characteristic of C–S–H. The ratio of the areas of  $Q_1$  to  $Q_2$  peaks can be calculated and leads to the mean length of the silicate chains. The mean length of the chains is 4.5 for  $\text{C}_3\text{S}$  hydrated without silica fume, and 5.5 for  $\text{C}_3\text{S}$  hydrated with silica fume.

The next step in acquiring knowledge of the C–S–H structure is the determination of the location and the number of protons.

In these materials, the interactions which broaden the lines in the NMR proton spectra are the homonuclear proton–proton dipolar interaction and the chemical shift interaction. The  $^1\text{H}$  MAS technique allows us to remove the effects of these interactions provided that the rotation frequency is higher than the frequency corresponding to the interaction to be removed.

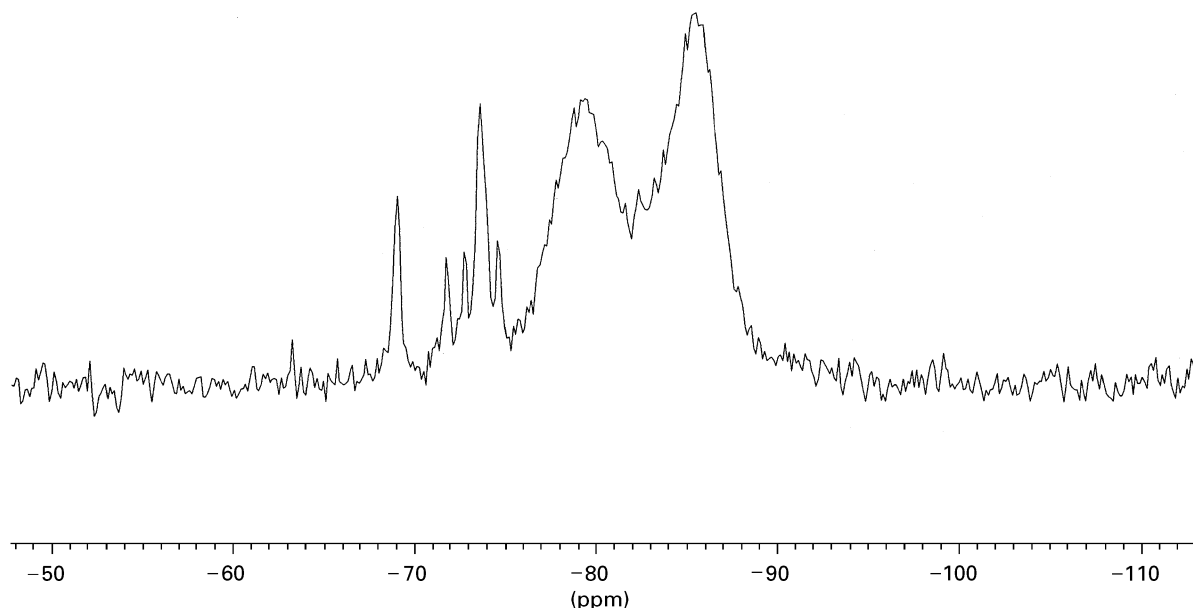


Figure 1  $^{29}\text{Si}$  NMR single-pulse spectrum of  $\text{C}_3\text{S}$  hydrated at  $120^\circ\text{C}$  for 24 h with the following acquisition parameters: a 59 MHz irradiation frequency, a rotor spinning speed of 4 kHz, a recycle delay of 150 s and 300 scans.

The combined rotation and multipulse spectroscopy (CRAMPS) technique is a NMR technique [3] which combines the MAS rotation of the sample with a multipulse sequence. This technique allows the removal of the interactions described above and leads to high-resolution proton spectra in solids. The rotation removes the effects of the chemical shift anisotropy while the multipulse sequence removes those of the dipolar interaction. It is therefore possible by  $^1\text{H}$  NMR to distinguish in the spectra the  $^1\text{H}$  lines corresponding to Ca–OH, Si–OH and H–OH groups in the studied samples and to estimate their population, the CRAMPS technique being a quantitative method.

The first  $^1\text{H}$  CRAMPS study of silicates was done by Heidemann [4, 5] and the range of isotropic  $^1\text{H}$  chemical shifts in crystalline hydrosilicates and inorganic hydrates was determined. This range is narrow (from  $-3$  to  $15$  ppm) in comparison with the range of  $^{29}\text{Si}$  chemical shifts (from  $-60$  to  $-120$  ppm) in the C–S–H. The first attempt in applying CRAMPS techniques to the study of poorly crystallized hydrates was made by Rassem *et al.* [6] on a 60 MHz spectrometer, but spectra were not well resolved.

Here we present, for the first time, well-resolved  $^1\text{H}$  CRAMPS NMR spectra of  $\text{C}_3\text{S}$  samples hydrated at  $120^\circ\text{C}$  with and without the presence of silica fume. The better resolution is probably due to an increased proton resonance frequency leading to an increased chemical shift separation (a 300 MHz spectrometer was used), a greater stability of the spectrometer and better adjustments. The previous study [1] has shown how the temperature rise leads to an acceleration of the  $\text{C}_3\text{S}$  hydration kinetics. At  $120^\circ\text{C}$ , a large number of hydrated species is obtained in a few days. We show how the CRAMPS technique, as a quantitative technique, is relevant to describe the different reactions occurring in a hydrating cement paste.

## 2. Experimental procedure

### 2.1. Sample preparation

Anhydrous  $\text{C}_3\text{S}$  was supplied by Ciments Français and its structure verified by X-ray diffraction. Dowell silica fume with a granulometry of  $15\ \mu\text{m}$  was used. Two types of sample were prepared:  $\text{C}_3\text{S}$  hydrated with silica fume and  $\text{C}_3\text{S}$  hydrated without silica fume. The samples of  $\text{C}_3\text{S}$  with silica fume were prepared with a silica-to- $\text{C}_3\text{S}$  weight ratio of 0.4 and a water-to-solid weight ratio of 0.55. The samples of  $\text{C}_3\text{S}$  without silica fume were prepared with a water-to-solid weight ratio of 0.44. The samples were synthesized at a temperature of  $120^\circ\text{C}$  under saturated steam pressure with an excess of water. In each case, three hydration times were studied: 24 h, 48 h and 7 days.

### 2.2. $^1\text{H}$ nuclear magnetic resonance with high-speed magic angle spinning

The experiments were carried out on a 500 MHz Bruker ASX spectrometer with a 4 mm MAS probe head which allows a rotation frequency of the sample up to 13 kHz. The following parameters were used: a  $90^\circ$  pulse length of  $6.5\ \mu\text{s}$ , a recycle time of 5 s and 400 scans.

### 2.3. $^1\text{H}$ combined rotation and multipulse spectroscopy nuclear magnetic resonance

A 300 MHz Bruker ASX spectrometer with a CRAMPS probe head was used. Rotors with a 7 mm diameter were specifically designed for CRAMPS. The sample was spinning at the magic angle at 2200 Hz. The following parameters were used: a multipulse BR24 CRAMPS sequence, a  $90^\circ$  pulse length of  $1.8\ \mu\text{s}$ , a recycle delay of 10 s and 100 scans. Adamantane was used to determine the scaling factor, which was 0.2.

Owing to stability problems of the spectrometer, adamantane was used as an internal reference. A single peak located at 1.74 ppm appears in the NMR spectrum of this product. Only one grain of adamantane inside the sample was needed to be observable in the CRAMPS NMR spectrum. For each sample, two spectra were acquired: one with the internal reference and one without. The spectrum with internal reference is used to calibrate the spectrum without internal reference which is used for quantitative measurements.

### 3. Results

#### 3.1. Static proton spectra

The static proton spectrum of the sample of  $C_3S$  hydrated with silica fume during 7 days at  $120^\circ C$  is shown in Fig. 2. This spectrum is the superposition of a very broad peak (with a linewidth of 20 kHz) and a narrower peak (with a linewidth of 5 kHz). The maximum of the narrower peak is located at 5.8 ppm, whereas the maximum of the broad peak is located at about 0.5 ppm. The spectra of the other samples present the same features.

#### 3.2. Proton magic angle spinning spectra

The spectrum of the sample of  $C_3S$  hydrated with silica fume for 7 days at  $120^\circ C$  acquired in MAS conditions is presented in Fig. 2. The rotation frequency is 10 kHz. At this frequency, the peak at 5.8 ppm of the static spectrum resolves into a peak with a linewidth of 2.5 kHz at 5.5 ppm and two narrow peaks at 2.2 ppm and 1.2 ppm.

These peaks are due to acetone and ether, which were used to stop sample hydration. The ether spec-

trum, acquired in a single-pulse  $^1H$  NMR sequence, shows two peaks at 3.5 ppm and at 1.2 ppm. Therefore one of the two fine peaks (1.2 ppm) in the MAS spectrum is due to ether, the other peak of ether (3.5 ppm) being obscured by the sharp peak at 5.5 ppm, and the second fine peak (2.2 ppm) is due to acetone (Fig. 2).

Spinning side bands from the peak at 0.5 ppm are observed. Our MAS probe head could not reach a frequency high enough to obtain complete resolution of the spectrum. In order to obtain a good resolution, we should reach a rotation speed of 20 kHz.

On the other hand, the  $^1H$  single-pulse spectrum of the empty probe head was acquired and subtracted from the MAS spectrum of the  $C_3S$  sample, a part of the broad peak in the MAS spectra is due to the protons of the probe head itself. Fig. 3 shows a spectrum without its probe-head component.

A MAS spectrum of the sample of  $C_3S$  hydrated at  $120^\circ C$  for 7 days acquired at different rotation frequencies is presented in Fig. 4. For a frequency of 4 kHz, the two narrow peaks begin to appear. The resolution is the same for MAS at 10 and 13 kHz.

#### 3.3. $^1H$ combined rotation and multipulse spectra

All  $^1H$  CRAMPS NMR spectra reveal two broad peaks located at 5.5 ppm and 0.5 ppm, as shown in Fig. 5, corresponding to the positions previously observed in the static spectra (Fig. 2). The linewidths at half-height are 1600 Hz (5.5 ppm peak) and 1000 Hz (0.5 ppm peak). The broad peak (20 kHz linewidth) observed in the static spectrum (Fig. 2) is well resolved now.

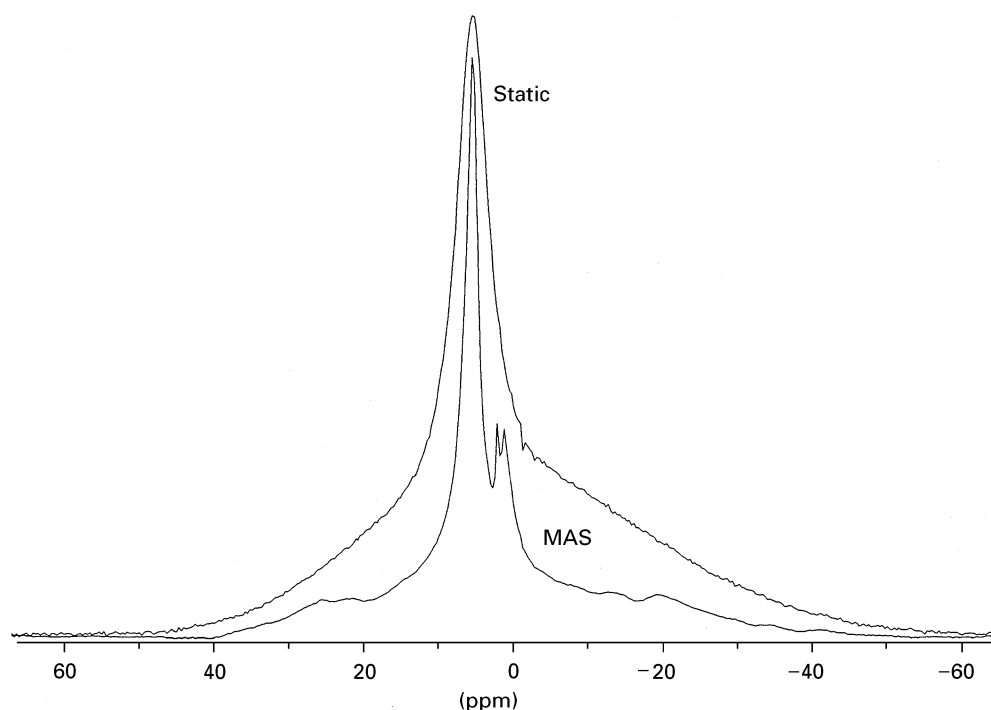


Figure 2 Superposition of a static proton NMR spectrum of  $C_3S$  hydrated at  $120^\circ C$  with silica fume for 7 days and the 10 kHz proton MAS NMR spectrum of this sample.

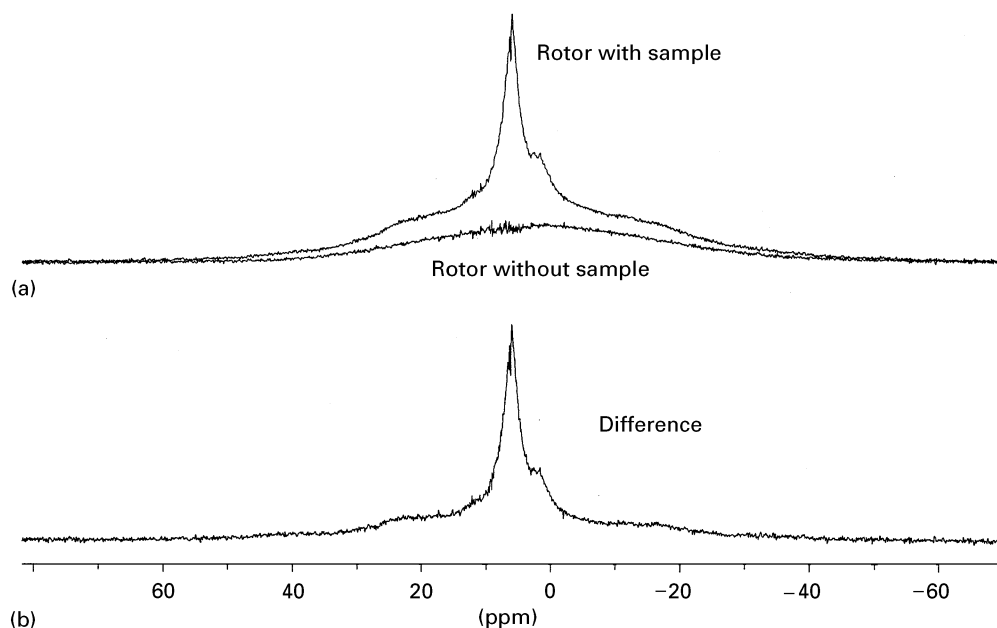


Figure 3 (a) MAS proton NMR spectrum (10 kHz) and probe-head component spectrum. (b) Difference between the two spectra.

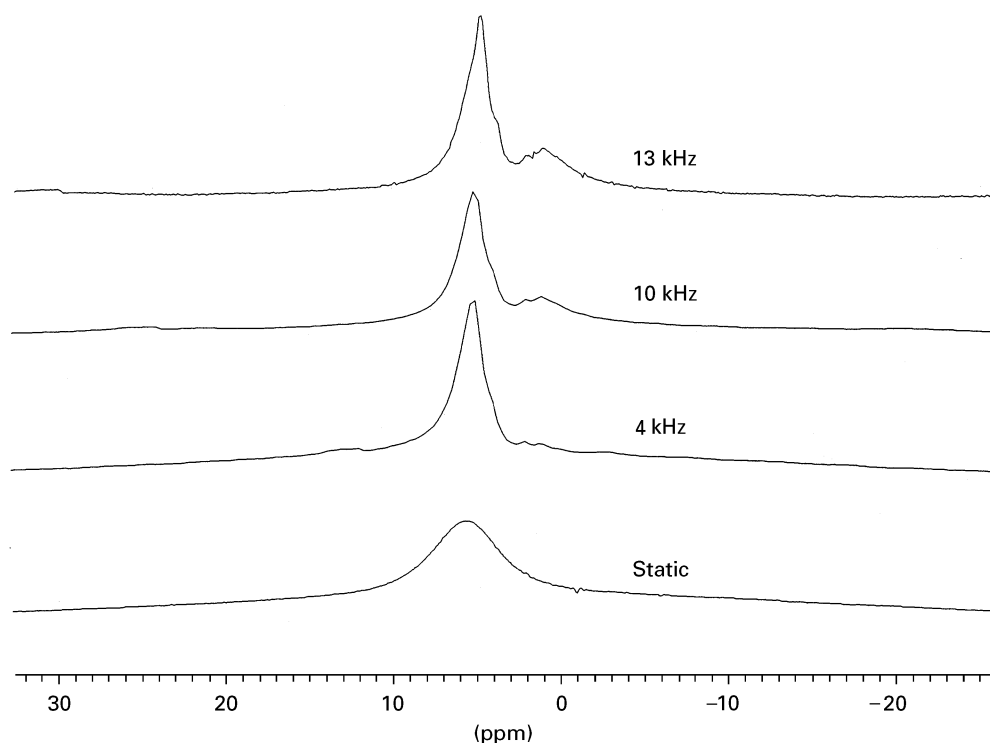


Figure 4 MAS NMR spectra at different rotation speeds of  $C_3S$  hydrated at  $120^\circ C$  for 7 days.

Using the range of  $^1H$  chemical shift established by Heidemann [4], the peak located at 0.5 ppm can be assigned to Ca–OH groups and the peak located at 5.5 ppm to Si–OH and H–OH groups. The proton numbers of each group can be compared, integrating the corresponding lines; however, the Si–OH and H–OH groups cannot be distinguished.

#### 4. Discussion

Comparison of a CRAMPS NMR spectrum and a high-speed MAS spectrum is made in Fig. 6 for the sample of  $C_3S$  hydrated with silica fume for 48 h. The

MAS technique, which reveals the two peaks of acetone and ether, does not allow us to obtain the resolution of the broad 20 kHz linewidth peak.

However, the CRAMPS NMR spectrum, acquired in too few scans to reveal acetone and ether peaks, clearly shows the difference between the number of Ca–OH groups and the number of Si–OH or H–OH groups.

The MAS spectrum and the CRAMPS NMR spectrum seem to be inconsistent (Fig. 6). However, as long as the MAS rotation frequency is lower than 20 kHz, no quantitative result can be extracted from the MAS spectrum, and CRAMPS NMR spectrum solely gives quantitative information.

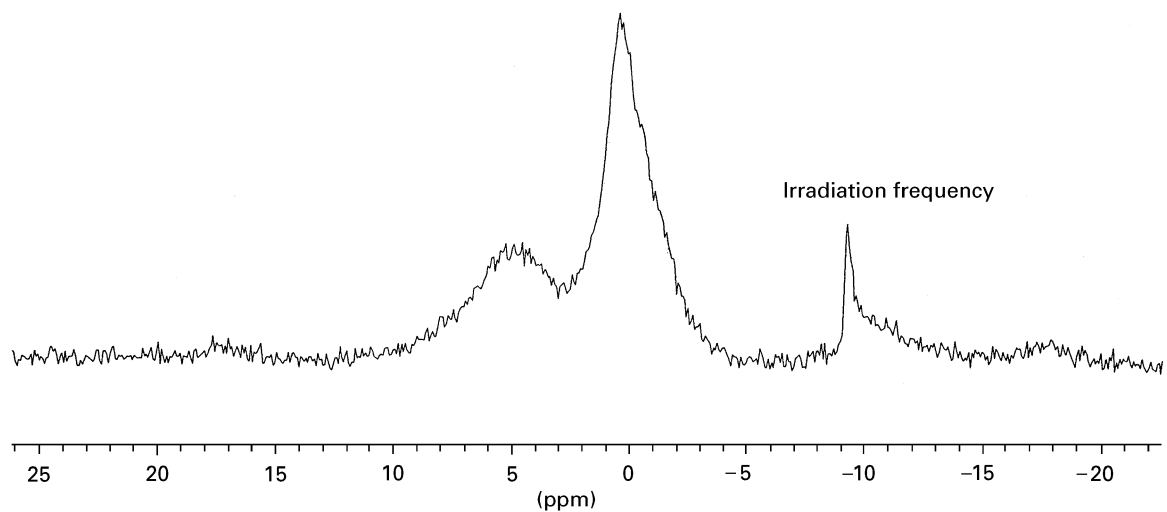


Figure 5 CRAMPS NMR spectrum of a sample of  $C_3S$  hydrated at  $120^\circ C$  without silica fume for 7 days.

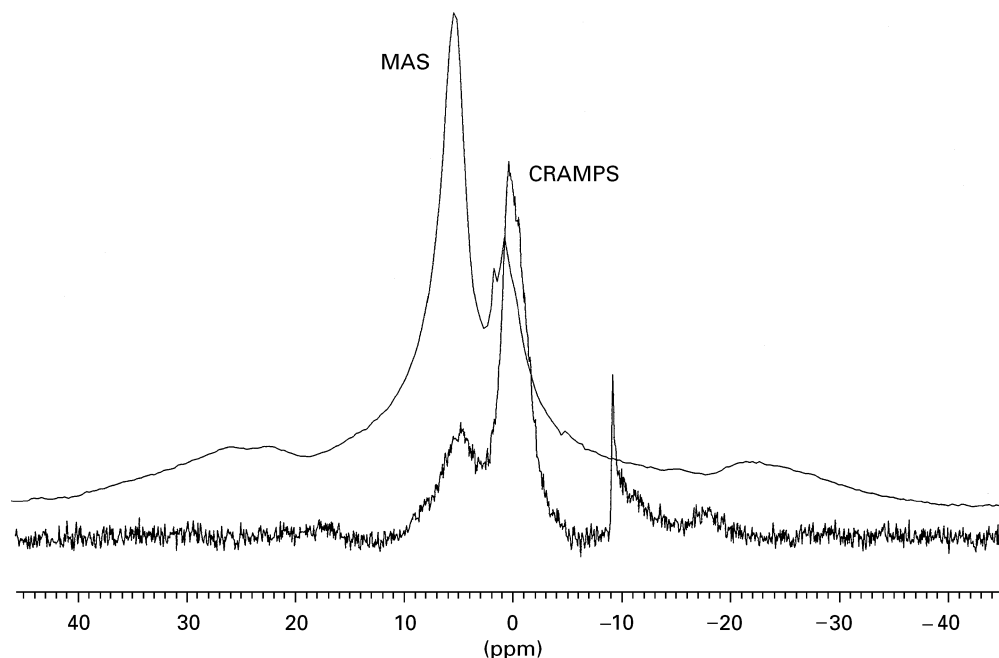


Figure 6 Comparison of MAS NMR (10 kHz) spectrum and CRAMPS NMR spectrum for a sample of  $C_3S$  hydrated at  $120^\circ C$  with silica fume for 48 h.

CRAMPS NMR spectra of all the samples are shown in Fig. 7. The scales are not absolute scales. All the spectra were deconvoluted in order to estimate each peak area. We call  $R$  the ratio  $[Ca-OH]/[Si-OH, H-OH]$ , where  $[Ca-OH]$  stands for the number of  $Ca-OH$  groups in the sample and  $[Si-OH, H-OH]$  stands for the number of  $Si-OH$  and  $H-OH$  groups in the sample. The results are presented in Table I.

After the same hydration time,  $R$ (without silica) is greater than  $R$ (with silica). The ratio  $R$ (without silica)/ $R$ (with silica) increases with increasing hydration time. Note that  $R$ (without silica) increases between 24 h and 48 h and remains constant between 48 h and 7 days. However,  $R$ (with silica) increases between 24 h and 48 h and decreases between 48 h and 7 days.

Different chemical mechanisms occur during the  $C_3S$  hydration with or without silica fume and are examined in order to interpret the spectra. They have been described for room temperature [7] and here we

shall suppose that the temperature essentially increases the kinetic of reactions.

In the case of  $C_3S$  hydration without silica fume,  $C_3S$  first dissolves, supplying three calcium ions for one silicate ion in the solution; a concentration gradient in calcium and silicate ions appears. When the solution is locally supersaturated in  $Ca^{2+}$  with respect to  $C-S-H$  (around the  $C_3S$  grain), this phase precipitates. All the supplied silicate ions are consumed by the  $C-S-H$  precipitation and growth, but the calcium concentration increases because of the  $C_3S$  dissolution. When the solution is locally supersaturated in  $Ca^{2+}$  with respect to portlandite, it also precipitates. The two hydrates grow around the  $C_3S$  grain. The amounts of portlandite and  $C-S-H$  increase with time. The dissolution of  $C_3S$  and the precipitation of portlandite and  $C-S-H$  occur simultaneously.

In the case of the  $C_3S$  hydration with silica fume, the same mechanisms occur. Precipitation of  $C-S-H$  and portlandite occur around the dissolving  $C_3S$  particle.

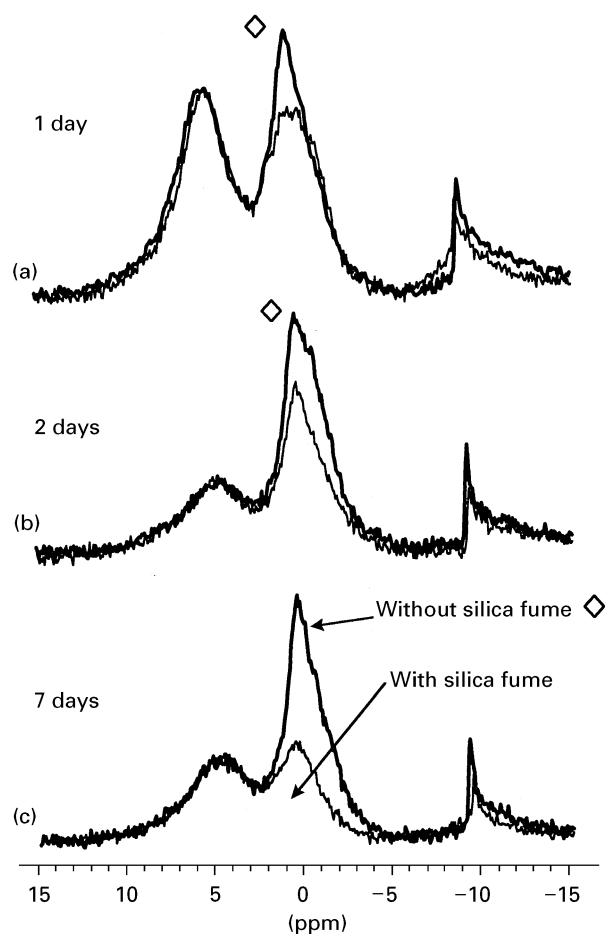


Figure 7 Comparison of CRAMPS NMR spectra of  $C_3S$  hydrated at  $120^\circ C$  with and without silica fume for (a) 1 day, (b) 2 days and (c) 3 days.

TABLE I Values of the ratio  $R$  (number of Ca–OH groups divided by the number of Si–OH and H–OH groups) with a  $\pm 0.1$  estimated error for different hydration times and for different samples

Hydration time	Hydration without silica fume	Hydration with silica fume
24 h	$R = 0.7$	$R = 0.6$
48 h	$R = 1.8$	$R = 1$
7 days	$R = 1.7$	$R = 0.4$

However, in this case the dissolution of silica fume particles leads to an increase in the silicate concentration in the neighbourhood of silica particles. A concentration gradient in silicate ions appears. According to [8], the C–S–H equilibrium curve of dissolution–precipitation depends on the silicate and calcium concentrations. The solution around the silica particles, with high silica concentration, leads to a C–S–H of lower calcium-to-silicon ratio  $[C]/[S]$  in the solid than the C–S–H near the  $C_3S$  grain [9]. As the hydration occurs, the layer of hydrates prevents the diffusion of calcium ions from the  $C_3S$  grain. Because of this lack of calcium ions, the solution in the neighbourhood of the silica grains becomes undersaturated with respect to portlandite; portlandite near the silica particles begins to dissolve. Two chemical processes are in competition; near the  $C_3S$  particles (which provide many calcium ions), portlandite and

C–S–H precipitate because of the higher calcium concentration. Near the silica particles, the higher silica concentration leads to the precipitation of a lower  $[C]/[S]$  C–S–H and dissolution of portlandite. According to [10], C–S–H formed in the neighbourhood of silica particles are more structured and have longer chain lengths than the remaining hydrates. When some Ca–OH groups disappear (as portlandite dissolves), other Ca–OH groups are formed in the two C–S–H (more or less rich in silica).

At an early stage of hydration (24 h),  $R$  is approximately the same in the case of  $C_3S$  hydration with or without silica fume. Until this stage of hydration, the kinetics of precipitation of portlandite dominates and the limiting mechanism is the silica dissolution.

Between 24 h and 48 h, in the case of  $C_3S$  hydration with silica fume, the two chemical processes (precipitation and dissolution of portlandite) begin to be in competition. After 48 h,  $R$  has increased in both cases, but  $R$ (without silica) is greater than  $R$ (with silica); portlandite grows less rapidly than in the case of  $C_3S$  hydration without silica.

Between 48 h and 7 days,  $R$ (without silica) remains constant because the reaction goes slowly. However,  $R$ (with silica) decreases because portlandite is consumed. The limiting mechanism is the migration of calcium ions through the layer of hydrates. In the case of  $C_3S$  hydrated for 7 days with silica fume, the X-ray diffraction shows that portlandite is completely consumed and  $R$  only corresponds to the C–S–H phase.

## 5. Conclusion

Two  $^1H$ NMR techniques (high-speed MAS and CRAMPS) have been used to study  $C_3S$  hydrated at  $120^\circ C$  with and without silica fume. The C–S–H phases and portlandite are the two main hydrates which precipitate during hydration. The MAS technique gives partially resolved spectra because the sample rotation speed is not high enough to remove the effects of the  $^1H$ – $^1H$  dipolar broadening (20 kHz) completely and side bands are observed. At the maximum speed which was available (13 kHz), no quantitative results can be deduced. Therefore the CRAMPS technique has been used. The signal acquired with the multipulse sequence can effectively remove the effect of dipolar broadening. The results obtain by CRAMPS are in agreement with the interpretation of the reactions which occur in hydrating paste. The spectra clearly show the effects of adding silica fume in the paste. They illustrate the competition between the two reactions which occur during  $C_3S$  hydration in presence of silica fume. Around the  $C_3S$  grain, the solution (which is rich in calcium ions) favours the precipitation of portlandite while, near the silica grains, portlandite tends to be consumed because of the presence of silica ions and a lack of calcium ions. Eventually, portlandite is completely consumed.

## Acknowledgement

The authors are grateful to Dr M. F. Quinton for her great help with the CRAMPS.

## References

1. S. MASSE, H. ZANNI, J. LECOURTIER, J. C. ROUSSEL and A. RIVEREAU, *J. Chim. Phys.* **92** (1995) 1861.
2. G. M. M. BELL, J. BENSTED, F. P. GLASSER, E. E. LACHOWSKI, D. R. ROBERTS and M. J. TAYLOR, *Adv. Cem. Res.* **3** (1990) 23.
3. B. C. GERSTEIN, R. G. PEMBLETON, R. C. WILSON and L. M. RYAN, *J. Chem. Phys.* **66** (1977) 361.
4. D. HEIDEMANN, Thesis, Akademie der Wissenschaften der BDR, Berlin (1987).
5. D. HEIDEMANN, in "Application of NMR spectroscopy to cement science," Guerville, March 1992, edited by P. Colombet and A. R. Grimmer (Gordon and Breach, Paris, 1994) p. 77.
6. R. RASSEM, H. ZANNI-THEVENEAU, D. HEIDEMANN and A. R. GRIMMER, *Cem. Concr. Res.* **23** (1993) 169.
7. C. VERNET, in "Application of NMR spectroscopy to cement science," Guerville, March 1992, edited by P. Colombet and A. R. Grimmer (Gordon and Breach, Paris, 1994) p. 29.
8. S. A. GREENBERG and T. N. CHANG, *J. Phys. Chem.* **69** (1965) 182.
9. H. UCHIKAWA, in "Proceedings of the Ninth International Congress on the Chemistry of Cement", New Delhi, 1992 (National Council for Cement and Building Materials, New Delhi, 1992) p. 797.
10. A. R. BROUGH, C. M. DOBSON, I. G. RICHARDSON and G. W. GROVES, *J. Mater. Sci.* **30** (1995) 1671.

*Received 5 March 1996  
and accepted 10 March 1997*